Title: Parsing multiomics landscape of activated synovial fibroblasts highlights drug targets linked to genetic risk of rheumatoid arthritis

Authors: Haruka Tsuchiya[1,†], Mineto Ota[1,2,3,†], Shuji Sumitomo[1], Kazuyoshi Ishigaki[4], Akari Suzuki[3], Toyonori Sakata[5], Yumi Tsuchida[1], Hiroshi Inui[8], Jun Hirose[8], Yuta Kochi[3,6], Yuho Kadono[7], Katsuhiko Shirahige[5], Sakae Tanaka[8], Kazuhiko Yamamoto[3], Keishi Fujio[1,*]

Affiliations:

[1]Department of Allergy and Rheumatology, Graduate School of Medicine, The University of Tokyo, Tokyo, 113-0033, Japan.

[2]Department of Functional Genomics and Immunological Diseases, Graduate School of Medicine, The University of Tokyo, Tokyo, 113-0033, Japan.

[3]Laboratory for Autoimmune Diseases, RIKEN Center for Integrative Medical Sciences, Yokohama, 230-0045, Japan.

[4]Divisions of Genetics and Rheumatology, Department of Medicine, Brigham and Women's Hospital, Harvard Medical School, Boston, MA 02115, USA.

[5]Laboratory of Genome Structure and Function, Institute for Quantitative Biosciences, The University of Tokyo, Tokyo, 113-0032, Japan.

[6]Department of Genomic Function and Diversity, Medical Research Institute, Tokyo Medical and

Dental University, Tokyo, 113-8510, Japan.

[7]Department of Orthopaedic Surgery, Saitama Medical University, Saitama, 350-0495, Japan.

[8]Department of Orthopaedic Surgery, Graduate School of Medicine, The University of Tokyo, Tokyo,

113-0033, Japan.

†These authors contributed equally

*Correspondence: K.F., kfujio-tky@umin.ac.jp

One Sentence Summary: SFs under synergistic inflammation is associated with RA heritability,

and MTF1 and RUNX1 could be crucial for the pathogenic chromatin rearrangement.

Abstract: In rheumatoid arthritis (RA), synovial fibroblasts (SFs) produce a variety of pathogenic

molecules in the inflamed synovium. Despite their potential importance, comprehensive genetic

network of SFs under inflammatory conditions remains elusive. Here, to elucidate the actions of SFs

and their contributions to RA pathogenesis, SFs, stimulated with 8 proinflammatory cytokines, were

analyzed using genomic, epigenomic and transcriptomic approaches. SFs exposed to synergistically

acting cytokines produced markedly higher levels of pathogenic molecules, including CD40 whose

expression was significantly affected by a RA risk SNP (rs6074022). Upon chromatin remodeling in

2

activated SFs, RA risk loci were enriched in clusters of enhancers (super-enhancers; SEs) induced by

synergistic proinflammatory cytokines. A RA risk SNP (rs28411362), located in a SE under

synergistically acting cytokines, formed three-dimensional contact with the promoter of *MTF1* gene,

whose binding motif showed significant enrichment in stimulation specific-SEs. Consistently,

inhibition of MTF1 suppressed cytokine and chemokine production from SFs and ameliorated mice

model of arthritis. These results demonstrates that integrative analysis of transformed SFs under the

inflammatory environment yields potential therapeutic targets associated with genetic risk of RA.

3

[Main Text:]

Introduction

Rheumatoid arthritis (RA) is an autoimmune disease that affects ~1% of the population worldwide and causes persistent synovial inflammation leading to disabling joint destruction. Current treatment strategies that target proinflammatory cytokines (e.g., TNF-α, IL-6), cell surface proteins of immune cells (e.g., CD20, CD80/86) or signaling molecules (e.g., JAK-STAT pathway) have brought a paradigm shift in RA treatment. However, achieving sustained remission is still challenging even with such agents (*1*). Although the concepts of targeting multiple molecules have been proposed to increase therapeutic efficacy, combination therapies (anti-TNF-α and anti-IL-1β or anti-IL-17) or bispecific antibodies (anti-TNF-α/IL-17) failed to achieve improved control (*2*). These findings imply that some unknown regulators of inflammation play critical roles in the progression of synovitis.

In the pathogenesis of RA, the activities of a variety of dysregulated molecules in immune cells (e.g., T cells, B cells, monocytes) and mesenchymal cells are orchestrated by genetic and environmental factors (*3*). Twin studies have estimated that the heritability of RA is as high as 60%, and more than 100 RA susceptibility loci have been identified in genome-wide association studies (GWAS) (*4*). Recent genetic studies of autoimmune diseases have reported that the majority (> 90%) of these risk variants are located in non-coding regions and regulate the expression levels of a

4

number of genes in a cell type-specific manner (*5*), partly in an environment-specific fashion (*6*). An

integrated understanding of the risk variants' contribution to gene regulatory networks is crucial to

determine the key molecules and cell types in RA pathogenesis.

Synovial fibroblasts (SFs) are the most abundant resident mesenchymal cells of the hyperplastic

synovium. They are major local effectors in the initiation and perpetuation of destructive joint

inflammation through their production of a variety of immunomodulators, adhesion molecules and

matrix-degrading enzymes (*3*). For example, SFs are a leading source of IL-6, a central hub in the

synovial cytokine network, and its receptor antagonist has shown efficacy for patients with RA (*7*). A

previous study conducted integrative analysis of transcriptomic and epigenomic data of unstimulated

SFs have addressed uncovering novel pathways activated in RA (*8*). However a comprehensive

picture of SFs' contribution to the pathogenesis of RA has largely remained elusive, perhaps due to

their complex features that change in response to the proinflammatory milieu (*9*). To date, a number

of cytokines that induce the inflammatory behavior of SFs have been reported (e.g., IFN-γ and IL-17

from T cells and TNF-α, IL-1β, IFN-α, IL-18 and TGF-β1 from monocytes) (*10*). These cytokines

activate various signaling pathways (e.g., nuclear factor-kappa B (NF-κB) signaling, Janus kinase

(JAK) signaling) *in vitro* that lead to the production of pathogenic molecules from SFs. To make

matters more complicated, in the setting of the inflamed synovium, SFs are expected to be exposed

to a more complex proinflammatory environment. Data show that some cytokine combinations (e.g.,

5

TNF-α and IL-17) (*11*) synergistically enhance the expression of cytokines and chemokines (e.g., IL-1, IL-6 and IL-8). Those findings emphasize the need to analyze the mechanisms underlying the accelerated inflammatory behavior of SFs in the presence of multiple synergistic factors.

Here, we used integrative methods to analyze genomic, transcriptomic and epigenomic features of RASFs in the presence of various proinflammatory cytokines that have been detected in RA joints (*12*). We demonstrate that SFs exposed to synergistic proinflammatory cytokines show distinct transcriptomic features characterized by elevated expression of pathogenic molecules (i.e., cytokines, chemokines and transcription factors) accompanied by chromatin remodeling associated with genetic risk of RA.

Results

Cytokine mixture induce a distinctive transcriptome signature in SFs

We stimulated SFs from RA and osteoarthritis (OA) patients (n=30 each) with 8 different cytokines (IFN-α, IFN-γ, TNF-α, IL-1β, IL-6/sIL-6R, IL-17, TGF-β1, IL-18) or a combination of all 8 (8-mix). We also fractionated peripheral blood mononuclear cells (PBMCs) from the same patients into five major immune cell subsets (CD4^{+} T cells, CD8^{+} T cells, B cells, NK cells, monocytes), which were not treated with the cytokines (Fig. 1).

Next, we quantified mRNA expression by RNA sequencing and compared transcriptome signatures

6

of SFs between the 10 conditions (i.e., non-stimulated, IFN-α, IFN-γ, TNF-α, IL-1β, IL-6/sIL-6R,

IL-17, TGF-β1, IL-18 or 8-mix) and the diseases (i.e., RA, OA). Principal component analysis

(PCA) of gene expression levels showed that the 8-mix condition induced a distinct transcriptome

signature compared with the other stimulatory conditions, corresponding to the first component (PC1

in Fig. 2A and fig. 2B). For instance, the markedly high expression of *IL6*, which codes a pivotal

cytokine in RA pathogenesis with a diverse repertoire of functions (e.g., osteoclast differentiation)

(*7*), was achieved by the 8-mix stimulation (Primary component loading on PC1 = -0.76, PC2 = 0.26.

Fig. 2C). Other genes coding cytokines that are associated with RA (e.g., *MMP3*, *CSF2*) were also

significantly upregulated when stimulated by the 8-mix combination (Fig. 2C). On the other hand,

RASFs showed different transcriptome signatures from OASFs under non-stimulatory or stimulatory

conditions, corresponding largely to the second component (PC2 in Fig. 2A and fig. 2B). Stimulation

by individual cytokines induced unique transcriptomic signatures in SFs (Fig. 2A and fig. 2B).

Recently, Fan Zhang and colleagues performed single-cell RNA sequencing analysis of RA and OA

synovial cells and reported that SFs could be clustered into 4 fractions (*13*). To elucidate the

association between transcriptional changes of SFs under cytokine stimulation and those 4 fractions,

we utilized the gene sets that Fan Zhang *et al.* reported were characteristic of each of the fractions.

We then scored our samples with these signatures (*14*) (Fig. S1). Interestingly, the signature score of

fraction 4, which was the population abundant in the lining of OA synovium in a previous report (*13*),

7

was higher in OASFs irrespective of the stimulatory conditions. In contrast, the score of fraction 2, which was a major *IL6* producer and abundant in the sublining of the RA synovium, was not different between RA and OA in non-stimulatory conditions, but they were strongly upregulated under IFN-γ, IFN-α, IL-6 or 8-mix stimulation. Accordingly, we surmised that certain SF populations were quantitatively stable among disease conditions, and some are inducible under cytokine stimulation.

eQTL effects of RA genetic risk loci are modulated by an environmental perturbation

We next performed cis-eQTL analysis to evaluate how transcription was affected by genetic variants in stimulated SFs and PBMC subsets. Together with tissue-by-tissue analysis, we also utilized Meta-Tissue software (Supplemental Materials), a linear mixed model that allows for heterogeneity in effect sizes across conditions, for a meta-analysis across SFs under 10 stimulatory conditions and 5 PBMC subsets. When we analyzed RA and OA samples separately, the eQTL effect sizes showed high similarities between RA and OA samples. To overcome the issue of modest sample sizes, we jointly analyzed the RA and OA samples for the following analyses. We considered variants with FDR < 0.1 in single tissue analysis or m-value > 0.9 in meta-analysis as significant eQTLs in line with previous reports (*15, 16*).

As a result, 3245 - 4118 genes in SFs and 2557 - 2828 genes in PBMCs had significant eQTLs

under each condition (Fig. S2A). In total, 6962 genes in SFs and 5043 genes in PBMCs had eQTLs

in at least one condition, and 2368 genes showed eQTL effects only in SFs (Fig. S2B). We note that

a substantial fraction of SF-specific eQTLs might be a consequence of low statistical power due to

limited sample size. However, we observed a distinguishable pattern of eQTLs in SFs from that of

PBMCs when comparing the effect sizes in meta-analysis (Fig. S2C), indicating a tissue-wise

difference of eQTL effects. When we focused on the effect size difference between stimulating SFs,

the 8-mix showed the smallest correlation coefficients compared with other conditions (Fig. S2C).

 Next, we examined candidate causal genes among GWAS loci in SFs. We focused on eQTL

variants with minimum *P* values in each associated eGene with meta-analysis or single tissue

analysis, which are in linkage disequilibrium (LD) with GWAS top-associated loci of RA. Notably,

various overlapped loci were observed in SFs (Table. S1). One example is rs6074022, which is in

tight LD ($r^2 = 0.95$ in EUR population, $r^2 = 0.9$ in EAS population) with an established RA risk locus

rs4810485 (*17*). By plotting eQTL meta-analysis posterior probability *m*-values and tissue-by-tissue

analysis -$\log_{10} P$ values, rs6074022 had robust eQTL effects on *CD40* in SFs, especially under 8-mix

or IFN-γ stimulatory conditions (Fig. 3A and fig. 3D). Importantly, the presence of an active

regulatory region at rs6074022 was inferred only under these stimulatory conditions (Fig. 3B).

Although *CD40* is also expressed by B cells (Fig. 3C) and known to be crucial for B cell activation

9

as a costimulatory protein (*18*), the eQTL effect at this locus was not observed in B cells in our study.

The biological role of the CD40-CD40L pathway in SFs has been discussed previously (*19, 20*). However, it has not been fully explained. We performed transcriptomic analysis of RASFs stimulated with a 2-trimer form of the CD40 ligand and IFN-γ. As a result, some chemokines (e.g., *CCL5*, *CXCL10*) and cytokines (e.g., *IL6*) were significantly upregulated by the ligation of CD40L (Fig. 3E). Taken together, we conjecture that CD40 upregulation in stimulated SFs is influenced by genetic predisposition, and the CD40-CD40L pathway might have a pathogenic role in RASFs.

Other example of eQTL-eGene pairs in SFs was rs7993214-*COG6*. The association of this locus and autoimmune diseases (RA, juvenile idiopathic arthritis and psoriasis) has been established (*21, 22*). The top eQTL variant of *COG6* in 8-mix-stimulated SFs or monocytes (rs7993214) was in tight LD with the GWAS top variant (rs9603616, $r^2 = 0.93$ in EUR population, $r^2 = 0.82$ in EAS population), and eQTL effects became more significant in stimulated SFs than in non-stimulated conditions.

FAM213B, located in an RA GWAS-associated region, also showed eQTL effect size heterogeneity under stimulation. *CD300E, SLAMF1* and *TRAF2*, which show stimulation specificity in eQTL effects, are shown in fig. S3. The eQTL variant list is available at the National Bioscience Database Center (NBDC) with the accession codes hum0207.v1.eQTL.v1.

10

Genetic risks of RA accumulate in the transcriptomic and epigenomic perturbations induced

by multiple cytokines

Next, in order to elucidate the link between RA genetic risks and transcriptomic perturbations of SFs

induced by various inflammatory conditions, we performed gene-set analysis with RA-associated

genetic loci using MAGMA software (Supplemental Materials), which computes gene-level trait

association scores and perform gene-set enrichment analysis of some gene sets with neighboring

genes in the risk loci. This analysis indicated that perturbed gene sets subject to IFN-α, IFN-γ and

8-mix cytokine stimulation significantly overlapped with RA risk loci ($P = 2.0 \times 10^{-4}$, 1.7×10^{-4} and

8.3×10^{-6}, respectively). Those data contrasted with the non-significant association of transcriptome

differences between RA and OA with RA genetic risk (Fig. S4A and fig. S4B). These findings

indicate that there is an accumulation of RA risk loci in the pathways that are perturbed under

specific stimulatory conditions in SFs from the perspective of transcriptomics.

  We also assessed the enrichment of RA top risk SNPs in regulatory regions including

super-enhancers (SEs) identified with ChIP sequencing. While the epigenomic mapping consortium

"Roadmap" has constructed a public database of human epigenome data

(http://www.roadmapepigenomics.org/), which is a fundamental resource for disease-epigenome

association analysis, few epigenomic data for SFs under stimulatory conditions are publicly

11

available. SEs are large clusters of transcriptional enhancers collectively bound by an array of

transcription factors to drive expression of genes that define cell identity (*23-25*). It is now known

that disease-associated variants are enriched in the SEs of disease-relevant cell types. Although the

significant overlap of SEs in Th cells and B cells with RA risk loci has been reported (*23*), SFs have

not been examined. Here we divided active enhancers into SEs and typical-enhancers (TEs)

following standard ROSE algorithms (Supplemental Materials) and compared the enrichment of RA

risk loci to epigenomic marks. Consistent with previous reports (*23*), RA risk loci showed significant

enrichment with SEs in CD4$^+$ T cells and B cells, as well as with SEs in 8-mix stimulated SFs from

RA or OA samples (Fig. 4A). SEs formed under different stimulatory conditions showed modest

overlap with RA risk loci. In contrast, 8-mix cytokine treatment showed the largest unique SE

overlap with some of the RA risk loci. (Fig. 4B and fig. 4C). When we performed a similar

comparison of our epigenomic data and risk loci for type 1 diabetes mellitus (a representative

example of non-articular autoimmune disease), only SEs in CD4$^+$ T cells and B cells showed

significant enrichment (Fig. S4C). The number or width of 8-mix SEs were not different from those

in non-stimulated or single cytokine stimulating SFs in total (Fig. S5). Consequently, SFs might

behave as key players in RA pathogenesis especially under synergistic inflammation.

SEs induced by cytokine mixtures regulate genes crucial for RA pathogenesis

12

Following the results above, we attempted to elucidate the genes regulated by 8-mix-enhanced SEs.

SEs are not necessarily located adjacent to transcription start sites (TSS). In fact, they may lie more

than 50 kb away from the TSS (*26*). First, to characterize the genes controlled by SEs, we combined

the 3D genome architectures (chromatin loops detected by Hi-C analysis), the position of SEs,

promoter regions (defined with H3K4me3 ChIP sequencing analysis) and genomic coordinates. We

annotated "SE-contacted genes" such that one side of Hi-C loop anchors overlapped a SE, the other

side of the loop coincided with the TSS of the gene and coexisted with the H3K4me3 peak (Fig. 5A).

SEs were more highly overlapped with Hi-C loop anchors than were TEs or H3K4me1 peaks (Fig.

S6A). H3K4me3 peaks also showed significant enrichment in Hi-C loop ends. When the gene TSS

and H3K27ac peak was connected by a Hi-C loop, the variation of mRNA expression showed a

significant correlation with the H3K27ac peak variation (Fig. S6B). These results underscore the

validity of connecting active enhancer marks and TSS by Hi-C loops in our dataset, as other reports

have shown (*27, 28*). When we compared the expression level of SE-contacted genes and

TE-contacted genes, the former showed significantly higher expression levels than the latter (Fig.

S6C), consistent with previous reports (*25*).

 Next, we compared genes contacted by either SEs or TEs of SFs under 3 different conditions:

nonstimulated SFs or those that were TNF-α-activated or stimulated by the mix of 8 factors. The

proportions of overlap between the 3 conditions were smaller in SE-contacted genes (9.7%) than

13

TE-contacted genes (14.5%) (Fig. 5B), indicating that the stimulation-specific gene expression profile and SEs formation. SE-contacted genes included a number of transcription factors (e.g., *MTF1, RUNX1*) and genes reported to play pathogenic roles in RA such as chemokines (e.g., *CCL5, CCL8*) and cytokines (e.g., *IL6*) (Fig. 5B and table. S2).

IL6 is a representative example of an 8-mix SE-contacted gene. Although this gene is regulated by a SE (almost 30 kb long) that exists upstream of the TSS in non-stimulated or TNF-α stimulated SFs, this SE elongates to 70 kb long under 8-mix conditions and an additional Hi-C loop emerges (Fig. 6A). As previously mentioned, *IL6* expression is markedly upregulated under 8-mix conditions (Fig. 2C), and when we inhibited SE formation with JQ1, a BRD4 inhibitor, the increased IL-6 expression under 8-mix conditions was reduced in a dose-dependent manner (Fig. 6B). The necessity of SEs for elevated IL-6 production under synergistic inflammation could be inferred from these findings.

Another example of an 8-mix SE-contacted gene is *Runt related transcription factor 1* (*RUNX1*) (Fig. 6C). *RUNX1* is a master-regulator transcription factor involved in normal and malignant hematopoiesis and in T-cell acute lymphoblastic leukemia. *RUNX1* is involved in the expression of critical oncogenes (e.g., *TAL1*) by binding to their SEs with other components of the leukemogenic transcriptional complex (e.g., *MYB*) (*29-31*). Additionally, the binding motif of *RUNX1* was enriched in SEs of synovial fluid-derived CD4^{+} T cells from juvenile idiopathic arthritis patients (*32*). In our study, RA risk locus rs8133843 overlapped with the 8-mix SE that exists upstream of *RUNX1*. A

Hi-C loop was formed with the promoter immediately above the second exon of *RUNX1* only in

8-mix conditions, and the *RUNX1* expression level was higher in the 8-mix condition compared with

others.

 Metal-regulatory transcription factor-1 (*MTF1*), a zinc finger transcription factor, which was

reported to be an essential catabolic regulator of OA pathogenesis and tumor progression (*33, 34*), is

another example of an 8-mix SE-contacted gene (Fig. 6E). *MTF1* expression was upregulated in the

8-mix condition (Fig. 6F). RA risk locus rs28411352 overlapped with an 8-mix SE that exists

upstream of the *MTF1*. The Hi-C loop was detected with the promoter only under the 8-mix

condition.

Transcription factors associated with stimulation-induced SE formation control arthritis

progression

Finally, we searched for candidate modulators that were crucial for SE formation, especially in the

8-mix condition. In the previous study, key transcription factors for SE formation were reported to

be controlled by SEs themselves, forming a self-regulatory network (*25*). From this perspective, we

used motif analysis to focus on SE-contacted transcription factors that were also enriched in SEs

under the 8-mix condition and compared them with TEs or SEs in the absence of stimulation (Fig.

7A). Among SE-contacted genes, transcription factors such as SNAI1, TCF4 and MTF1 showed

15

significant motif enrichment in 8-mix SEs. MTF1 was the only example that also showed the overlap of 8-mix SE and RA GWAS risk variant as discussed above (Fig. 6E). Although the RUNX1 motif was not enriched in 8-mix SEs compared with unstimulated SEs, its motif was significantly enriched in SEs compared with the background sequence, both in 8-mix conditions and without stimulation ($P = 1.0 \times 10^{-16}$ and 1.0×10^{-20}, respectively). When these transcription factors in RASFs were silenced with siRNAs, the expression of 8-mix SE-contacted genes was significantly suppressed by *MTF1* and *RUNX1* knockdown ($P = 2.0 \times 10^{-3}$ and 4.3×10^{-4}, respectively) (Fig. 7B and fig. S7). The effect of *MTF1* knockdown was more pronounced in 8-mix SE-contacted genes than TE-contacted genes. In *in vitro* assay, the increased representative 8-mix SE-contacted gene expressions (IL-6, CCL5) from RASFs under 8-mix conditions was reduced by treatment with APTO-253, a MTF1 inhibitor (*35*) (Fig. 7C and fig. 7D). Furthermore, in a collagen induced arthritis (CIA) model, APTO-253 demonstrated significant preventive (Fig. S8) and therapeutic activity (Fig. 7E and fig. 7F) on arthritis formation. Collectively, these results indicated that certain transcription factors, including MTF1 and RUNX1, play critical roles in the formation of inflammation–associated epigenomic structures in the presence of synergistic cytokines, and support MTF1 inhibition as a promising therapy candidate for RA (Fig. 8).

Discussion

16

In this study, we conducted integrated analyses of SFs from Japanese RA and OA patients. Under

stimulation with a combination of proinflammatory cytokines, we were able to describe the dynamic

landscape of SFs and their contribution to RA pathogenesis. SFs under the influence of synergistic

cytokines exhibited a distinct transcriptome signature characterized by high expression of pathogenic

genes (e.g., *IL6*, *MMP3*, *CSF2*). These findings were in line with the reported synergistic

inflammatory responses of SFs to leukocyte-derived cytokines (TNF-α and IL-17). For example,

specifically induced modulators (CUX1 and IκBζ) engage the NF-κB complex to upregulate certain

chemokines (*36*).

 Recent large-scale eQTL studies analyzing the function of non-coding variants enhanced our

understanding of complex diseases (*37, 38*). Considering the importance of studying disease-relevant

tissues for functional understanding of GWAS variants (*15, 39*), we expanded previous eQTL

studies through analyses of SFs, which are major local effector cells in arthritic joints. To our

knowledge, this study is the first to conduct cis-eQTL analysis of SFs. Using cis-eQTL analysis, we

identified thousands of associated eGenes in SFs, some of which showed the heterogeneous sizes of

effects under different stimulatory conditions. One example was the association of an RA risk locus

(rs4810485) with *CD40* expression. Although no significant eQTL effects of this locus in B cells

was observed in our data, a previous report showed the protein-level QTL association of CD40 in

CD19^{+} B cells and this locus in European seropositive RA patients and controls (*40*). On the

17

contrary, a larger eQTL study by the GTEx consortium that showed genome-wide significant eQTL effects of rs6074022 on CD40 in lung (mainly fibroblasts) ($P = 3.1 \times 10^{-26}$) and cultured fibroblasts ($P = 8.4 \times 10^{-16}$), but not in EBV-transformed lymphocytes ($P = 0.04$). The subtle gap in results could be derived from racial differences of study populations and study design. Naturally, although the possible importance of CD40 signals in B cells for RA pathogenesis cannot be neglected, our result of eQTL analysis and functional study in SFs shed light on the role of CD40-CD40L signals in a genetic network of synovial inflammation.

 The significance of synergistic interactions between proinflammatory cytokines and SFs is supported by the observed accumulation of RA genetic risk loci as shown by transcriptomic and epigenomic data obtained under specific stimulatory conditions. SEs control molecules that have prominent roles in cell type-specific processes, and are hotspots for disease susceptibility (*23-25*). The GWAS-SEs enrichment analysis shows that SFs can behave as pathogenic cells in the development of RA (analogous to CD4$^+$ T cells and B cells) especially when exposed to the synergistic activity of proinflammatory cytokines. Note that the positions of SEs are highly flexible, and they can shift during cell differentiation or activation (*41-43*). Indeed, we found that SEs in SFs shifted during stimulation. The significant enrichment of RA risk SNPs in the SEs in SFs under 8-mix stimulation suggests that susceptibility regions could be exposed to the transcriptional machinery. Furthermore, recent fine chromatin contact maps revealed that SEs are in close proximity

18

to the promoter of the gene they activate (*44-47*). During synergistic cytokine stimulation, Hi-C

analysis suggested that there were dynamic conformational changes in three-dimensional structures

involving SEs and the promoter of pathological molecules (i.e., cytokines, chemokines and

transcription factors). We found marked expression of 8-mix stimulated SE-contacted genes (i.e.,

IL6, *RUNX1*, *MTF1*).

SEs can collapse when their co-factors are perturbed (*48*). Those cofactors include BET family

members (Brd2, Brd3, Brd4 and Brdt) that bind to acetylated lysines in histone tails and

transcription factors. In cancers that acquire SEs to drive expression of prominent oncogenes (*48*),

BRD4 inhibitors (i.e., JQ1) ameliorated tumor progression *in vitro* and *in vivo* (*49*). BRD4 silencing

also reduced cytokine secretion, migration and invasion activity of RASFs, and JQ1 ameliorated

arthritis in a collagen-induced arthritis model (*50*). On the other hand, selective modulation of SEs

that preferentially target disease-associated SEs in a cell type-specific manner may have better safety

profiles than pan-SEs inhibitors (i.e., JQ1). In T cell leukemias, a small monoallelic insertion creates

binding motifs for the master transcription factor MYB, which trigger SEs initiation upstream of

oncogenes (*30*).

In the present study, we analyzed transcription factors that have the potential to be selective SE

modulators in SFs when stimulated by multiple synergistic proinflammatory cytokines. The *in vitro*

knockdown assay revealed that silencing of *MTF1* or *RUNX1* significantly suppressed SE-contacted

19

genes in the presence of 8 cytokines. Moreover, the effect of *MTF1* silencing was more prominent in

8-mix SE-contacted genes than TE-contacted genes. Those results suggest that MTF1 participates in

SE formation, putatively making a feedback loop to maintain the epigenomic machinery. MTF1, a

zinc finger transcription factor, regulates gene expression by binding to the metal regulatory element

(MRE) within the promoter of downstream genes, in response to zinc and various stresses (*51*). In

the setting of disease, MTF1 could contribute to tumor metastasis and chemoresistance in some

cancer cells (*52*). APTO-253, a MTF1 inhibitor (*35*), is a small molecule with antitumor activity

against a wide range of human malignancies in *in vitro* and in xenograft mouse models (*53, 54*). In

the present study, APTO-253 demonstrated inhibitory activity on the expression of pathogenic

molecules (IL-6, CCL5) from RASFs exposed to synergistic cytokines and antiarthritic activity in a

CIA model. Previously, the zinc-ZIP8-MTF1 axis was identified as a catabolic regulator of cartilage

destruction (*33*). In OA chondrocytes, the Zn^{++} importer ZIP8 is specifically upregulated, and the

resulting Zn^{++} influx activates MTF1, thereby enhancing the expression of matrix-degrading

enzymes. Furthermore, intra-articular injection of adenovirus expressing-MTF1 in an experimental

mouse model of OA promoted the expression of various matrix-degrading enzymes, cytokines and

chemokines in SFs. This evidence supports the essential role of MTF1 as a genetic hub for joint

destruction and inflammation.

There are some limitations of this study. First, the number of patients included in the cis-eQTL analysis was limited owing to sample accessibility, resulting in putatively large false negatives. Increased sample size could better reveal the genetic influences on stimulated SFs. Second, SFs were purified by a conventional method, that is, serial passage. Previous reports showed that passage number could affect the epigenome and transcriptome of SFs (*55, 56*). To minimize the impact of culture, we restricted our analysis to early passage cells. Third, PBMCs in the present study were freshly isolated by flow cytometry and were not artificially stimulated with cytokines *ex vivo*. Thus, it is not clear whether the eQTL difference between SFs and PBMCs is attributable to cell type difference. However, over 80% of RA patients had moderate to high disease activity at the time of blood sampling, indicating that PBMCs were subject to a proinflammatory environment.

Overall, our findings shed light on activated SFs and their role in RA heritability. We also examined the conformational dynamics of chromatin fibers as related to the amplification of inflammation given a genetic predisposition. Our data suggest the concept of SF-targeted therapy from the perspective of epigenome remodeling. Transcription factors (MTF1, RUNX1) preferentially recruited to SEs during exposure to multiple synergistic proinflammatory cytokines would constitute novel drug targets.

21

Materials and Methods

Study Design

The overall objectives were to explore the actions of SFs in the presence of various proinflammatory cytokines and their contributions to RA pathogenesis. We quantified mRNA expression by RNA sequencing and compared transcriptome of SFs between the 10 conditions (i.e., non-stimulated, IFN-α, IFN-γ, TNF-α, IL-1β, IL-6/sIL-6R, IL-17, TGF-β1, IL-18 or 8-mix) and the diseases (i.e., RA, OA). We also performed an cis-eQTL analysis to evaluate how transcription was affected in stimulated SFs and five major immune cell subsets (CD4$^+$ T cells, CD8$^+$ T cells, B cells, NK cells, monocytes) from the same patient, and we examined candidate causal genes among GWAS loci in SFs. Focusing on eQTL variants in LD with GWAS top-associated loci of RA, we assessed the biological role of the CD40-CD40L pathway in SFs by transcriptomic analysis of RASFs stimulated with a 2-trimer form of the CD40 ligand and IFN-γ as a representative example. Furthermore, to elucidate the link between genetic risk of RA and transcriptomic or epigenomic perturbations of stimulated SFs, we performed a gene level enrichment analysis with RA-associated genetic loci. We also assessed the overlap of RA top risk SNPs with two types of regulatory regions (SEs or TEs) identified with ChIP sequencing. In addition, we searched for candidate modulators crucial for SE formation, especially in the 8-mix condition. To this end, we characterized SE-contacted regulatory factors by combining the 3D genome architectures (chromatin loops detected by Hi-C analysis), the

position of SEs and promoter regions (defined with H3K4me3 ChIP sequencing analysis), integrated with motif analysis. Last, the promising pathogenic transcription factors in RASFs were silenced with siRNAs, and the effect of MTF1 inhibitor was assessed by *in vitro* and *in vivo*.

Additional materials and methods are available in the Supplementary Materials.

Human Participants and Sample Collection

Synovial tissues were obtained from RA and OA patients (n = 30 each) undergoing joint replacement surgery at the University of Tokyo Hospital, Japan. RA patients fulfilled the 2010 ACR/EULAR (American College of Rheumatology/European League Against Rheumatism) criteria for the classification of RA (*57*). Patient characteristics are summarized in Table. S4. This study was approved by the Ethics Committees of the University of Tokyo (G3582), RIKEN and the indicated medical institutions. Written informed consent was obtained from each subject in accordance with the Declaration of Helsinki. Fresh synovial tissues were minced and digested with 0.1% collagenase (Worthington) at 37□, in 5% CO_2 for 1.5 h and SFs were cultured in Dulbecco's modified Eagle's medium (DMEM; SIGMA) supplemented with 10% fetal bovine serum (FBS; BioWest), 100 µg/mL L-glutamine, 100 U/mL penicillin, 100 µg/mL streptomycin (all from Invitrogen). SFs from passage 2 or 3 were used for RNA sequencing, ChIP sequencing, Hi-C and functional studies after removal of macrophages by magnetic separation with CD14 microbeads (Miltenyi Biotec). The purity of SFs

23

was tested by flow cytometry analysis (MoFlo XDP; Beckman Coulter). SFs were stained with CD14-, Thy-1 (CD90)-specific monoclonal antibodies (clone IDs: M5E2, 5E10, respectively, all from BioLegend). Most cells (>99%) had the surface marker for fibroblasts (Thy-1) but not CD14.

We collected peripheral blood from the same patients. PBMCs were isolated using Ficoll-Paque density gradient centrifugation followed by staining with CD3-, CD4-, CD8-, CD14-, CD19-, and CD56-specific monoclonal antibodies (clone IDs: UCHT1, OKT4, RPA-T8, M5E2, HIB19 and HCD56, respectively, all from BioLegend). Five immune cell populations were sorted by flow cytometry (MoFlo XDP; Beckman Coulter) using the following gating strategy: $CD4^+$ T cells: $CD3^+CD4^+CD8^-CD19^-$; $CD8^+$ T cells: $CD3^+CD4^-CD8^+CD19^-$; B cells: $CD3^-CD19^+$; NK cells: $CD3^-CD14^-CD19^-CD56^+$; and monocytes: $CD3^-CD14^+CD19^-$. There were 3×10^5 cells in each population.

Mice and Induction of CIA

DBA/1J male mice (6 weeks) were purchased from Japan SLC. To induce CIA, bovine type II collagen (CII; Chondrex) was emulsified in equal volume of Complete Freund's Adjuvant (CFA; Chondrex). Mice were intradermally injected with the emulsion (100 µL) containing 100 µg CII. Twenty-one days later, a secondary injection was given at the same concentration of CII emulsified in Incomplete Freudn's Adjuvant (IFA; Chondrex). Mice were examined every day for clinical signs

of arthritis after the first injection. The severity of arthritis was assessed by qualitative clinical score

determined as follows: 0 = normal paw; 1 =one toe inflamed and swollen; 2 = >1 toe, but not entire

paw inflamed and swollen, or mild swelling of entire paw; 3 = entire paw inflamed and swollen; 4 =

very inflamed and swollen or ankylosed paw. Each paw was scored individually, and totaled them

for each mouse (a maximum of 16 points). All procedures were performed in accordance with

National Institutes of Health (NIH) Guide for the Care and Use of Laboratory Animals and approved

by the ethics committee of the University of Tokyo Institutional Animal Care and Use Committee.

Statistical Analysis

For *in vitro* analysis, statistical significance and analysis of variance (ANOVA) between indicated

groups were analyzed by R (ver 3.4.1). A comparison of more than 2 group means was analyzed by

Tukey's multiple comparison tests. A comparison of 2 group means was analyzed by paired t-test or

Mann–Whitney U test. Statistically significant differences were accepted at $P < 0.05$ for all tests.

Data in the bar charts were expressed as means ± standard errors of the means (SEM).

Supplementary Materials

Materials and methods

Fig. S1. The Estimated Enrichment of SF Populations Revealed by Single-cell RNA Sequencing

Analysis of Freshly Isolated SFs.

Fig. S2. Summary of the Result of cis-eQTL Analysis in Stimulating SFs and PBMCs from RA and

OA patients.

Fig. S3. Representative Examples of eQTL in Stimulating SFs.

Fig. S4. Polygenic Association between Differentially Expressed Genes and RA Risk Variants, and

GWAS-Super-enhancers Enrichment Analysis in the Other Immune Related Disease.

Fig. S5. Comparison of the number and width of SEs between stimulatory conditions of SFs.

Fig. S6. The Relevance among Hi-C loop, SEs and Gene Expression Levels.

Fig. S7. Transcription Factors Associated with SEs Formation in 8-mix SFs.

Fig. S8. Preventive effect of APTO-253 on CIA in a DBA/1 J mouse model.

Fig. S9. A Graphical summary of the present study.

Table. S1. Colocalization of RA GWAS and eQTL signals (Separate file).

Table. S2. Summary of SE-connecting genes (Separate file).

Table. S3. Sequences of primer pairs used in qRT-PCR.

Table. S4. Characteristics of patients for RNA sequencing.

References and Notes:

1.   R. van Vollenhoven, Treat-to-target in rheumatoid arthritis - are we there yet? *Nature reviews. Rheumatology* **15**, 180-186 (2019).

2.   K. F. Baker, J. D. Isaacs, Novel therapies for immune-mediated inflammatory diseases: What can we learn from their use in rheumatoid arthritis, spondyloarthritis, systemic lupus erythematosus, psoriasis, Crohn's disease and ulcerative colitis? *Annals of the rheumatic diseases* **77**, 175-187 (2018).

3.   Z. Chen, A. Bozec, A. Ramming, G. Schett, Anti-inflammatory and immune-regulatory cytokines in rheumatoid arthritis. *Nature reviews. Rheumatology* **15**, 9-17 (2019).

4.   Y. Okada, D. Wu, G. Trynka, T. Raj, C. Terao, K. Ikari, Y. Kochi, K. Ohmura, A. Suzuki, S. Yoshida, R. R. Graham, A. Manoharan, W. Ortmann, T. Bhangale, J. C. Denny, R. J. Carroll, A. E. Eyler, J. D. Greenberg, J. M. Kremer, D. A. Pappas, L. Jiang, J. Yin, L. Ye, D. F. Su, J. Yang, G. Xie, E. Keystone, H. J. Westra, T. Esko, A. Metspalu, X. Zhou, N. Gupta, D. Mirel, E. A. Stahl, D. Diogo, J. Cui, K. Liao, M. H. Guo, K. Myouzen, T. Kawaguchi, M. J. Coenen, P. L. van Riel, M. A. van de Laar, H. J. Guchelaar, T. W. Huizinga, P. Dieude, X. Mariette, S. L. Bridges, Jr., A. Zhernakova, R. E. Toes, P. P. Tak, C. Miceli-Richard, S. Y. Bang, H. S. Lee, J. Martin, M. A. Gonzalez-Gay, L. Rodriguez-Rodriguez, S. Rantapaa-Dahlqvist, L. Arlestig, H. K. Choi, Y. Kamatani, P. Galan, M. Lathrop, S. Eyre, J.

27

Bowes, A. Barton, N. de Vries, L. W. Moreland, L. A. Criswell, E. W. Karlson, A. Taniguchi,

R. Yamada, M. Kubo, J. S. Liu, S. C. Bae, J. Worthington, L. Padyukov, L. Klareskog, P. K.

Gregersen, S. Raychaudhuri, B. E. Stranger, P. L. De Jager, L. Franke, P. M. Visscher, M. A.

Brown, H. Yamanaka, T. Mimori, A. Takahashi, H. Xu, T. W. Behrens, K. A. Siminovitch, S.

Momohara, F. Matsuda, K. Yamamoto, R. M. Plenge, Genetics of rheumatoid arthritis

contributes to biology and drug discovery. *Nature* **506**, 376-381 (2014).

5.   K. K. Farh, A. Marson, J. Zhu, M. Kleinewietfeld, W. J. Housley, S. Beik, N. Shoresh, H.

Whitton, R. J. Ryan, A. A. Shishkin, M. Hatan, M. J. Carrasco-Alfonso, D. Mayer, C. J.

Luckey, N. A. Patsopoulos, P. L. De Jager, V. K. Kuchroo, C. B. Epstein, M. J. Daly, D. A.

Hafler, B. E. Bernstein, Genetic and epigenetic fine mapping of causal autoimmune disease

variants. *Nature* **518**, 337-343 (2015).

6.   B. P. Fairfax, P. Humburg, S. Makino, V. Naranbhai, D. Wong, E. Lau, L. Jostins, K. Plant,

R. Andrews, C. McGee, J. C. Knight, Innate immune activity conditions the effect of

regulatory variants upon monocyte gene expression. *Science (New York, N.Y.)* **343**, 1246949

(2014).

7.   S. Kang, T. Tanaka, M. Narazaki, T. Kishimoto, Targeting Interleukin-6 Signaling in Clinic.

Immunity **50**, 1007-1023 (2019).

8.   R. Ai, T. Laragione, D. Hammaker, D. L. Boyle, A. Wildberg, K. Maeshima, E.

28

Palescandolo, V. Krishna, D. Pocalyko, J. W. Whitaker, Y. Bai, S. Nagpal, K. E. Bachman, R. I. Ainsworth, M. Wang, B. Ding, P. S. Gulko, W. Wang, G. S. Firestein, Comprehensive epigenetic landscape of rheumatoid arthritis fibroblast-like synoviocytes. *Nature communications* **9**, 1921 (2018).

9.   K. Slowikowski, K. Wei, M. B. Brenner, S. Raychaudhuri, Functional genomics of stromal cells in chronic inflammatory diseases. *Current opinion in rheumatology* **30**, 65-71 (2018).

10.   M. T. Leech, E. F. Morand, Fibroblasts and synovial immunity. *Current opinion in pharmacology* **13**, 565-569 (2013).

11.   Y. Katz, O. Nadiv, Y. Beer, Interleukin-17 enhances tumor necrosis factor alpha-induced synthesis of interleukins 1,6, and 8 in skin and synovial fibroblasts: a possible role as a "fine-tuning cytokine" in inflammation processes. *Arthritis and rheumatism* **44**, 2176-2184 (2001).

12.   W. P. Arend, J. M. Dayer, Cytokines and cytokine inhibitors or antagonists in rheumatoid arthritis. *Arthritis and rheumatism* **33**, 305-315 (1990).

13.   F. Zhang, K. Wei, K. Slowikowski, C. Y. Fonseka, D. A. Rao, S. Kelly, S. M. Goodman, D. Tabechian, L. B. Hughes, K. Salomon-Escoto, G. F. M. Watts, A. H. Jonsson, J. Rangel-Moreno, N. Meednu, C. Rozo, W. Apruzzese, T. M. Eisenhaure, D. J. Lieb, D. L. Boyle, A. M. Mandelin, 2nd, B. F. Boyce, E. DiCarlo, E. M. Gravallese, P. K. Gregersen, L.

Moreland, G. S. Firestein, N. Hacohen, C. Nusbaum, J. A. Lederer, H. Perlman, C. Pitzalis,

A. Filer, V. M. Holers, V. P. Bykerk, L. T. Donlin, J. H. Anolik, M. B. Brenner, S.

Raychaudhuri, Defining inflammatory cell states in rheumatoid arthritis joint synovial

tissues by integrating single-cell transcriptomics and mass cytometry. *Nature immunology*

20, 928-942 (2019).

14.   S. Hanzelmann, R. Castelo, J. Guinney, GSVA: gene set variation analysis for microarray

and RNA-seq data. *BMC bioinformatics* **14**, 7 (2013).

15.   E. R. Gamazon, A. V. Segre, M. van de Bunt, X. Wen, H. S. Xi, F. Hormozdiari, H. Ongen,

A. Konkashbaev, E. M. Derks, F. Aguet, J. Quan, D. L. Nicolae, E. Eskin, M. Kellis, G.

Getz, M. I. McCarthy, E. T. Dermitzakis, N. J. Cox, K. G. Ardlie, Using an atlas of gene

regulation across 44 human tissues to inform complex disease- and trait-associated variation.

Nature genetics **50**, 956-967 (2018).

16.   J. H. Sul, B. Han, C. Ye, T. Choi, E. Eskin, Effectively identifying eQTLs from multiple

tissues by combining mixed model and meta-analytic approaches. *PLoS genetics* **9**,

e1003491 (2013).

17.   S. Raychaudhuri, E. F. Remmers, A. T. Lee, R. Hackett, C. Guiducci, N. P. Burtt, L.

Gianniny, B. D. Korman, L. Padyukov, F. A. Kurreeman, M. Chang, J. J. Catanese, B. Ding,

S. Wong, A. H. van der Helm-van Mil, B. M. Neale, J. Coblyn, J. Cui, P. P. Tak, G. J.

Wolbink, J. B. Crusius, I. E. van der Horst-Bruinsma, L. A. Criswell, C. I. Amos, M. F.

Seldin, D. L. Kastner, K. G. Ardlie, L. Alfredsson, K. H. Costenbader, D. Altshuler, T. W.

Huizinga, N. A. Shadick, M. E. Weinblatt, N. de Vries, J. Worthington, M. Seielstad, R. E.

Toes, E. W. Karlson, A. B. Begovich, L. Klareskog, P. K. Gregersen, M. J. Daly, R. M.

Plenge, Common variants at CD40 and other loci confer risk of rheumatoid arthritis. *Nature*

genetics **40**, 1216-1223 (2008).

18.   J. L. Karnell, S. A. Rieder, R. Ettinger, R. Kolbeck, Targeting the CD40-CD40L pathway in

autoimmune diseases: Humoral immunity and beyond. *Advanced drug delivery reviews* **141**,

92-103 (2019).

19.   M. L. Cho, B. Y. Yoon, J. H. Ju, Y. O. Jung, J. Y. Jhun, M. K. Park, S. H. Park, C. S. Cho, H.

Y. Kim, Expression of CCR2A, an isoform of MCP-1 receptor, is increased by MCP-1,

CD40 ligand and TGF-beta in fibroblast like synoviocytes of patients with RA.

Experimental & molecular medicine **39**, 499-507 (2007).

20.   K. W. Kim, M. L. Cho, H. R. Kim, J. H. Ju, M. K. Park, H. J. Oh, J. S. Kim, S. H. Park, S. H.

Lee, H. Y. Kim, Up-regulation of stromal cell-derived factor 1 (CXCL12) production in

rheumatoid synovial fibroblasts through interactions with T lymphocytes: role of

interleukin-17 and CD40L-CD40 interaction. *Arthritis and rheumatism* **56**, 1076-1086

(2007).

21.   A. Hinks, J. Cobb, M. C. Marion, S. Prahalad, M. Sudman, J. Bowes, P. Martin, M. E. Comeau, S. Sajuthi, R. Andrews, M. Brown, W. M. Chen, P. Concannon, P. Deloukas, S. Edkins, S. Eyre, P. M. Gaffney, S. L. Guthery, J. M. Guthridge, S. E. Hunt, J. A. James, M. Keddache, K. L. Moser, P. A. Nigrovic, S. Onengut-Gumuscu, M. L. Onslow, C. D. Rose, S. S. Rich, K. J. Steel, E. K. Wakeland, C. A. Wallace, L. R. Wedderburn, P. Woo, J. F. Bohnsack, J. P. Haas, D. N. Glass, C. D. Langefeld, W. Thomson, S. D. Thompson, Dense genotyping of immune-related disease regions identifies 14 new susceptibility loci for juvenile idiopathic arthritis. *Nature genetics* **45**, 664-669 (2013).

22.   Y. Liu, C. Helms, W. Liao, L. C. Zaba, S. Duan, J. Gardner, C. Wise, A. Miner, M. J. Malloy, C. R. Pullinger, J. P. Kane, S. Saccone, J. Worthington, I. Bruce, P. Y. Kwok, A. Menter, J. Krueger, A. Barton, N. L. Saccone, A. M. Bowcock, A genome-wide association study of psoriasis and psoriatic arthritis identifies new disease loci. *PLoS genetics* **4**, e1000041 (2008).

23.   D. Hnisz, B. J. Abraham, T. I. Lee, A. Lau, V. Saint-Andre, A. A. Sigova, H. A. Hoke, R. A. Young, Super-enhancers in the control of cell identity and disease. *Cell* **155**, 934-947 (2013).

24.   A. Kundaje, W. Meuleman, J. Ernst, M. Bilenky, A. Yen, A. Heravi-Moussavi, P. Kheradpour, Z. Zhang, J. Wang, M. J. Ziller, V. Amin, J. W. Whitaker, M. D. Schultz, L. D.

Ward, A. Sarkar, G. Quon, R. S. Sandstrom, M. L. Eaton, Y. C. Wu, A. R. Pfenning, X. Wang, M. Claussnitzer, Y. Liu, C. Coarfa, R. A. Harris, N. Shoresh, C. B. Epstein, E. Gjoneska, D. Leung, W. Xie, R. D. Hawkins, R. Lister, C. Hong, P. Gascard, A. J. Mungall, R. Moore, E. Chuah, A. Tam, T. K. Canfield, R. S. Hansen, R. Kaul, P. J. Sabo, M. S. Bansal, A. Carles, J. R. Dixon, K. H. Farh, S. Feizi, R. Karlic, A. R. Kim, A. Kulkarni, D. Li, R. Lowdon, G. Elliott, T. R. Mercer, S. J. Neph, V. Onuchic, P. Polak, N. Rajagopal, P. Ray, R. C. Sallari, K. T. Siebenthall, N. A. Sinnott-Armstrong, M. Stevens, R. E. Thurman, J. Wu, B. Zhang, X. Zhou, A. E. Beaudet, L. A. Boyer, P. L. De Jager, P. J. Farnham, S. J. Fisher, D. Haussler, S. J. Jones, W. Li, M. A. Marra, M. T. McManus, S. Sunyaev, J. A. Thomson, T. D. Tlsty, L. H. Tsai, W. Wang, R. A. Waterland, M. Q. Zhang, L. H. Chadwick, B. E. Bernstein, J. F. Costello, J. R. Ecker, M. Hirst, A. Meissner, A. Milosavljevic, B. Ren, J. A. Stamatoyannopoulos, T. Wang, M. Kellis, Integrative analysis of 111 reference human epigenomes. *Nature* **518**, 317-330 (2015).

25.   W. A. Whyte, D. A. Orlando, D. Hnisz, B. J. Abraham, C. Y. Lin, M. H. Kagey, P. B. Rahl, T. I. Lee, R. A. Young, Master transcription factors and mediator establish super-enhancers at key cell identity genes. *Cell* **153**, 307-319 (2013).

26.   A. Khan, A. Mathelier, X. Zhang, Super-enhancers are transcriptionally more active and cell type-specific than stretch enhancers. *Epigenetics* **13**, 910-922 (2018).

27.   O. Delaneau, M. Zazhytska, C. Borel, G. Giannuzzi, G. Rey, C. Howald, S. Kumar, H. Ongen, K. Popadin, D. Marbach, G. Ambrosini, D. Bielser, D. Hacker, L. Romano, P. Ribaux, M. Wiederkehr, E. Falconnet, P. Bucher, S. Bergmann, S. E. Antonarakis, A. Reymond, E. T. Dermitzakis, Chromatin three-dimensional interactions mediate genetic effects on gene expression. *Science (New York, N.Y.)* **364**,   (2019).

28.   M. R. Mumbach, A. T. Satpathy, E. A. Boyle, C. Dai, B. G. Gowen, S. W. Cho, M. L. Nguyen, A. J. Rubin, J. M. Granja, K. R. Kazane, Y. Wei, T. Nguyen, P. G. Greenside, M. R. Corces, J. Tycko, D. R. Simeonov, N. Suliman, R. Li, J. Xu, R. A. Flynn, A. Kundaje, P. A. Khavari, A. Marson, J. E. Corn, T. Quertermous, W. J. Greenleaf, H. Y. Chang, Enhancer connectome in primary human cells identifies target genes of disease-associated DNA elements. *Nature genetics* **49**, 1602-1612 (2017).

29.   C. Bahr, L. von Paleske, V. V. Uslu, S. Remeseiro, N. Takayama, S. W. Ng, A. Murison, K. Langenfeld, M. Petretich, R. Scognamiglio, P. Zeisberger, A. S. Benk, I. Amit, P. W. Zandstra, M. Lupien, J. E. Dick, A. Trumpp, F. Spitz, A Myc enhancer cluster regulates normal and leukaemic haematopoietic stem cell hierarchies. *Nature* **553**, 515-520 (2018).

30.   M. R. Mansour, B. J. Abraham, L. Anders, A. Berezovskaya, A. Gutierrez, A. D. Durbin, J. Etchin, L. Lawton, S. E. Sallan, L. B. Silverman, M. L. Loh, S. P. Hunger, T. Sanda, R. A. Young, A. T. Look, Oncogene regulation. An oncogenic super-enhancer formed through

somatic mutation of a noncoding intergenic element. *Science (New York, N.Y.)* **346**, 1373-1377 (2014).

31.   C. P. Mill, W. Fiskus, C. D. DiNardo, Y. Qian, K. Raina, K. Rajapakshe, D. Perera, C. Coarfa, T. M. Kadia, J. D. Khoury, D. T. Saenz, D. N. Saenz, A. Illendula, K. Takahashi, S. M. Kornblau, M. R. Green, A. P. Futreal, J. H. Bushweller, C. M. Crews, K. N. Bhalla, RUNX1-targeted therapy for AML expressing somatic or germline mutation in RUNX1. *Blood* **134**, 59-73 (2019).

32.   J. G. Peeters, S. J. Vervoort, S. C. Tan, G. Mijnheer, S. de Roock, S. J. Vastert, E. E. Nieuwenhuis, F. van Wijk, B. J. Prakken, M. P. Creyghton, P. J. Coffer, M. Mokry, J. van Loosdregt, Inhibition of Super-Enhancer Activity in Autoinflammatory Site-Derived T Cells Reduces Disease-Associated Gene Expression. *Cell reports* **12**, 1986-1996 (2015).

33.   J. H. Kim, J. Jeon, M. Shin, Y. Won, M. Lee, J. S. Kwak, G. Lee, J. Rhee, J. H. Ryu, C. H. Chun, J. S. Chun, Regulation of the catabolic cascade in osteoarthritis by the zinc-ZIP8-MTF1 axis. *Cell* **156**, 730-743 (2014).

34.   B. J. Murphy, Regulation of malignant progression by the hypoxia-sensitive transcription factors HIF-1alpha and MTF-1. *Comparative biochemistry and physiology. Part B, Biochemistry & molecular biology* **139**, 495-507 (2004).

35.   H. U. Osmanbeyoglu, F. Shimizu, A. Rynne-Vidal, D. Alonso-Curbelo, H. A. Chen, H. Y.

Wen, T. L. Yeung, P. Jelinic, P. Razavi, S. W. Lowe, S. C. Mok, G. Chiosis, D. A. Levine, C. S. Leslie, Chromatin-informed inference of transcriptional programs in gynecologic and basal breast cancers. *Nature communications* **10**, 4369 (2019).

36.   K. Slowikowski, H. N. Nguyen, E. H. Noss, D. P. Simmons, F. Mizoguchi, G. F. M. Watts, M. F. Gurish, M. B. Brenner, S. Raychaudhuri, CUX1 and IκBζ mediate the synergistic inflammatory response to TNF and IL-17A in stromal fibroblasts. *bioRxiv*, 571315 (2019).

37.   A. Battle, C. D. Brown, B. E. Engelhardt, S. B. Montgomery, Genetic effects on gene expression across human tissues. *Nature* **550**, 204-213 (2017).

38.   T. Lappalainen, M. Sammeth, M. R. Friedlander, P. A. t Hoen, J. Monlong, M. A. Rivas, M. Gonzalez-Porta, N. Kurbatova, T. Griebel, P. G. Ferreira, M. Barann, T. Wieland, L. Greger, M. van Iterson, J. Almlof, P. Ribeca, I. Pulyakhina, D. Esser, T. Giger, A. Tikhonov, M. Sultan, G. Bertier, D. G. MacArthur, M. Lek, E. Lizano, H. P. Buermans, I. Padioleau, T. Schwarzmayr, O. Karlberg, H. Ongen, H. Kilpinen, S. Beltran, M. Gut, K. Kahlem, V. Amstislavskiy, O. Stegle, M. Pirinen, S. B. Montgomery, P. Donnelly, M. I. McCarthy, P. Flicek, T. M. Strom, H. Lehrach, S. Schreiber, R. Sudbrak, A. Carracedo, S. E. Antonarakis, R. Hasler, A. C. Syvanen, G. J. van Ommen, A. Brazma, T. Meitinger, P. Rosenstiel, R. Guigo, I. G. Gut, X. Estivill, E. T. Dermitzakis, Transcriptome and genome sequencing uncovers functional variation in humans. *Nature* **501**, 506-511 (2013).

39.   M. Wainberg, N. Sinnott-Armstrong, N. Mancuso, A. N. Barbeira, D. A. Knowles, D. Golan,

R. Ermel, A. Ruusalepp, T. Quertermous, K. Hao, J. L. M. Bjorkegren, H. K. Im, B.

Pasaniuc, M. A. Rivas, A. Kundaje, Opportunities and challenges for transcriptome-wide

association studies. *Nature genetics* **51**, 592-599 (2019).

40.   G. Li, D. Diogo, D. Wu, J. Spoonamore, V. Dancik, L. Franke, F. Kurreeman, E. J. Rossin,

G. Duclos, C. Hartland, X. Zhou, K. Li, J. Liu, P. L. De Jager, K. A. Siminovitch, A.

Zhernakova, S. Raychaudhuri, J. Bowes, S. Eyre, L. Padyukov, P. K. Gregersen, J.

Worthington, N. Gupta, P. A. Clemons, E. Stahl, N. Tolliday, R. M. Plenge, Human genetics

in rheumatoid arthritis guides a high-throughput drug screen of the CD40 signaling pathway.

PLoS genetics **9**, e1003487 (2013).

41.   J. D. Brown, C. Y. Lin, Q. Duan, G. Griffin, A. Federation, R. M. Paranal, S. Bair, G.

Newton, A. Lichtman, A. Kung, T. Yang, H. Wang, F. W. Luscinskas, K. Croce, J. E.

Bradner, J. Plutzky, NF-kappaB directs dynamic super enhancer formation in inflammation

and atherogenesis. *Molecular cell* **56**, 219-231 (2014).

42.   N. Hah, C. Benner, L. W. Chong, R. T. Yu, M. Downes, R. M. Evans,

Inflammation-sensitive super enhancers form domains of coordinately regulated enhancer

RNAs. *Proceedings of the National Academy of Sciences of the United States of America*

112, E297-302 (2015).

43.   S. V. Schmidt, W. Krebs, T. Ulas, J. Xue, K. Bassler, P. Gunther, A. L. Hardt, H. Schultze, J. Sander, K. Klee, H. Theis, M. Kraut, M. Beyer, J. L. Schultze, The transcriptional regulator network of human inflammatory macrophages is defined by open chromatin. *Cell research* **26**, 151-170 (2016).

44.   J. M. Dowen, Z. P. Fan, D. Hnisz, G. Ren, B. J. Abraham, L. N. Zhang, A. S. Weintraub, J. Schujiers, T. I. Lee, K. Zhao, R. A. Young, Control of cell identity genes occurs in insulated neighborhoods in mammalian chromosomes. *Cell* **159**, 374-387 (2014).

45.   D. Hnisz, A. S. Weintraub, D. S. Day, A. L. Valton, R. O. Bak, C. H. Li, J. Goldmann, B. R. Lajoie, Z. P. Fan, A. A. Sigova, J. Reddy, D. Borges-Rivera, T. I. Lee, R. Jaenisch, M. H. Porteus, J. Dekker, R. A. Young, Activation of proto-oncogenes by disruption of chromosome neighborhoods. *Science (New York, N.Y.)* **351**, 1454-1458 (2016).

46.   X. Ji, D. B. Dadon, B. E. Powell, Z. P. Fan, D. Borges-Rivera, S. Shachar, A. S. Weintraub, D. Hnisz, G. Pegoraro, T. I. Lee, T. Misteli, R. Jaenisch, R. A. Young, 3D Chromosome Regulatory Landscape of Human Pluripotent Cells. *Cell stem cell* **18**, 262-275 (2016).

47.   K. R. Kieffer-Kwon, Z. Tang, E. Mathe, J. Qian, M. H. Sung, G. Li, W. Resch, S. Baek, N. Pruett, L. Grontved, L. Vian, S. Nelson, H. Zare, O. Hakim, D. Reyon, A. Yamane, H. Nakahashi, A. L. Kovalchuk, J. Zou, J. K. Joung, V. Sartorelli, C. L. Wei, X. Ruan, G. L. Hager, Y. Ruan, R. Casellas, Interactome maps of mouse gene regulatory domains reveal

basic principles of transcriptional regulation. *Cell* **155**, 1507-1520 (2013).

48.   J. Loven, H. A. Hoke, C. Y. Lin, A. Lau, D. A. Orlando, C. R. Vakoc, J. E. Bradner, T. I. Lee,

        R. A. Young, Selective inhibition of tumor oncogenes by disruption of super-enhancers. *Cell*

        153, 320-334 (2013).

49.   Y. X. See, B. Z. Wang, M. J. Fullwood, Chromatin Interactions and Regulatory Elements in

        Cancer: From Bench to Bedside. *Trends in genetics : TIG* **35**, 145-158 (2019).

50.   Q. G. Zhang, J. Qian, Y. C. Zhu, Targeting bromodomain-containing protein 4 (BRD4)

        benefits rheumatoid arthritis. *Immunology letters* **166**, 103-108 (2015).

51.   V. Gunther, U. Lindert, W. Schaffner, The taste of heavy metals: gene regulation by MTF-1.

        Biochimica et biophysica acta **1823**, 1416-1425 (2012).

52.   L. Ji, G. Zhao, P. Zhang, W. Huo, P. Dong, H. Watari, L. Jia, L. M. Pfeffer, J. Yue, J. Zheng,

        Knockout of MTF1 Inhibits the Epithelial to Mesenchymal Transition in Ovarian Cancer

        Cells. *Journal of Cancer* **9**, 4578-4585 (2018).

53.   A. Local, H. Zhang, K. D. Benbatoul, P. Folger, X. Sheng, C. Y. Tsai, S. B. Howell, W. G.

        Rice, APTO-253 Stabilizes G-quadruplex DNA, Inhibits MYC Expression, and Induces

        DNA Damage in Acute Myeloid Leukemia Cells. *Molecular cancer therapeutics* **17**,

        1177-1186 (2018).

54.   C. Y. Tsai, S. Sun, H. Zhang, A. Local, Y. Su, L. A. Gross, W. G. Rice, S. B. Howell,

APTO-253 Is a New Addition to the Repertoire of Drugs that Can Exploit DNA BRCA1/2 Deficiency. *Molecular cancer therapeutics* **17**, 1167-1176 (2018).

55. C. L. Galligan, E. Baig, V. Bykerk, E. C. Keystone, E. N. Fish, Distinctive gene expression signatures in rheumatoid arthritis synovial tissue fibroblast cells: correlates with disease activity. *Genes and immunity* **8**, 480-491 (2007).

56. J. W. Whitaker, R. Shoemaker, D. L. Boyle, J. Hillman, D. Anderson, W. Wang, G. S. Firestein, An imprinted rheumatoid arthritis methylome signature reflects pathogenic phenotype. *Genome medicine* **5**, 40 (2013).

57. D. Aletaha, T. Neogi, A. J. Silman, J. Funovits, D. T. Felson, C. O. Bingham, 3rd, N. S. Birnbaum, G. R. Burmester, V. P. Bykerk, M. D. Cohen, B. Combe, K. H. Costenbader, M. Dougados, P. Emery, G. Ferraccioli, J. M. Hazes, K. Hobbs, T. W. Huizinga, A. Kavanaugh, J. Kay, T. K. Kvien, T. Laing, P. Mease, H. A. Menard, L. W. Moreland, R. L. Naden, T. Pincus, J. S. Smolen, E. Stanislawska-Biernat, D. Symmons, P. P. Tak, K. S. Upchurch, J. Vencovsky, F. Wolfe, G. Hawker, 2010 Rheumatoid arthritis classification criteria: an American College of Rheumatology/European League Against Rheumatism collaborative initiative. *Arthritis and rheumatism* **62**, 2569-2581 (2010).

58. GTEx Consortium, Human genomics. The Genotype-Tissue Expression (GTEx) pilot analysis: multitissue gene regulation in humans. *Science (New York, N.Y.)* **348**, 648-660

(2015).

59. S. G. Landt, G. K. Marinov, A. Kundaje, P. Kheradpour, F. Pauli, S. Batzoglou, B. E.
Bernstein, P. Bickel, J. B. Brown, P. Cayting, Y. Chen, G. DeSalvo, C. Epstein, K. I.
Fisher-Aylor, G. Euskirchen, M. Gerstein, J. Gertz, A. J. Hartemink, M. M. Hoffman, V. R.
Iyer, Y. L. Jung, S. Karmakar, M. Kellis, P. V. Kharchenko, Q. Li, T. Liu, X. S. Liu, L. Ma,
A. Milosavljevic, R. M. Myers, P. J. Park, M. J. Pazin, M. D. Perry, D. Raha, T. E. Reddy, J.
Rozowsky, N. Shoresh, A. Sidow, M. Slattery, J. A. Stamatoyannopoulos, M. Y. Tolstorukov,
K. P. White, S. Xi, P. J. Farnham, J. D. Lieb, B. J. Wold, M. Snyder, ChIP-seq guidelines
and practices of the ENCODE and modENCODE consortia. *Genome research* **22**,
1813-1831 (2012).

60. S. S. Rao, M. H. Huntley, N. C. Durand, E. K. Stamenova, I. D. Bochkov, J. T. Robinson, A.
L. Sanborn, I. Machol, A. D. Omer, E. S. Lander, E. L. Aiden, A 3D map of the human
genome at kilobase resolution reveals principles of chromatin looping. *Cell* **159**, 1665-1680
(2014).

61. A. Buniello, J. A. L. MacArthur, M. Cerezo, L. W. Harris, J. Hayhurst, C. Malangone, A.
McMahon, J. Morales, E. Mountjoy, E. Sollis, D. Suveges, O. Vrousgou, P. L. Whetzel, R.
Amode, J. A. Guillen, H. S. Riat, S. J. Trevanion, P. Hall, H. Junkins, P. Flicek, T. Burdett, L.
A. Hindorff, F. Cunningham, H. Parkinson, The NHGRI-EBI GWAS Catalog of published

genome-wide association studies, targeted arrays and summary statistics 2019. *Nucleic*

acids research **47**, D1005-d1012 (2019).

hum0207.v1.eQTL.v1; peaks data of ChIP sequencing, hum0207.v1.ChIP.v1; chromatin loops data

of Hi-C, hum0207.v1.HiC.v1).
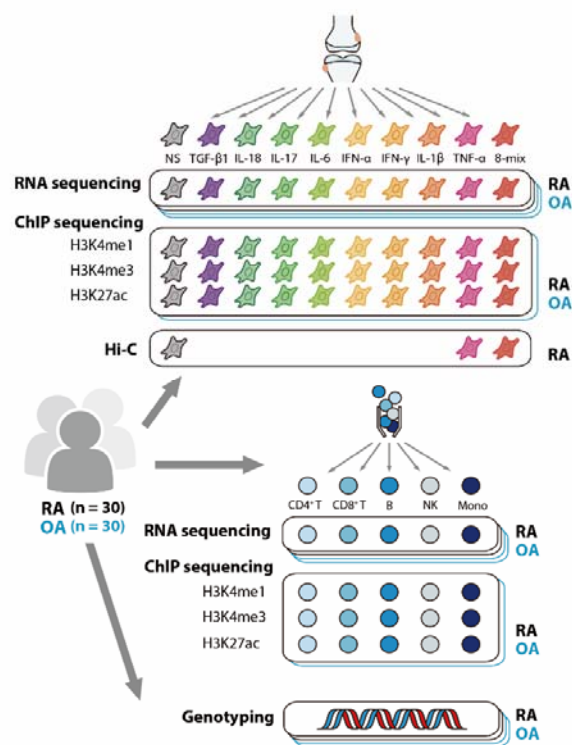
Figures:

Fig. 1. Experimental design for integrative analysis of stimulated SFs from RA and OA patients.

Our study design included SFs stimulated by 8 different factors plus a combination of all the factors. Specifically, cells were treated for 24 h with one of the following: IFN-α 100 U/mL, IFN-γ 200 U/mL, TNF-α 10 ng/mL, IL-1β 10 ng/mL, IL-6/sIL-6R 200 ng/mL, IL-17 10 ng/mL, TGF-β1 10 ng/mL or IL-18 100 ng/mL or 8-mix, a mixture of the above 8 cytokines. In addition, we used 5 freshly isolated PBMC populations (CD4^{+} T cells, CD8^{+} T cells, B cells, NK cells, monocytes) from

45

the same patient cohort. RNA sequencing of individual samples from RA and OA patients (n=30 per

each) was carried out, and ChIP sequencing and Hi-C analysis were conducted with pooled samples.

SNP genotyping array was performed in all patients.

SFs, synovial fibroblasts; PBMCs, peripheral blood mononuclear cells; RA, rheumatoid arthritis;

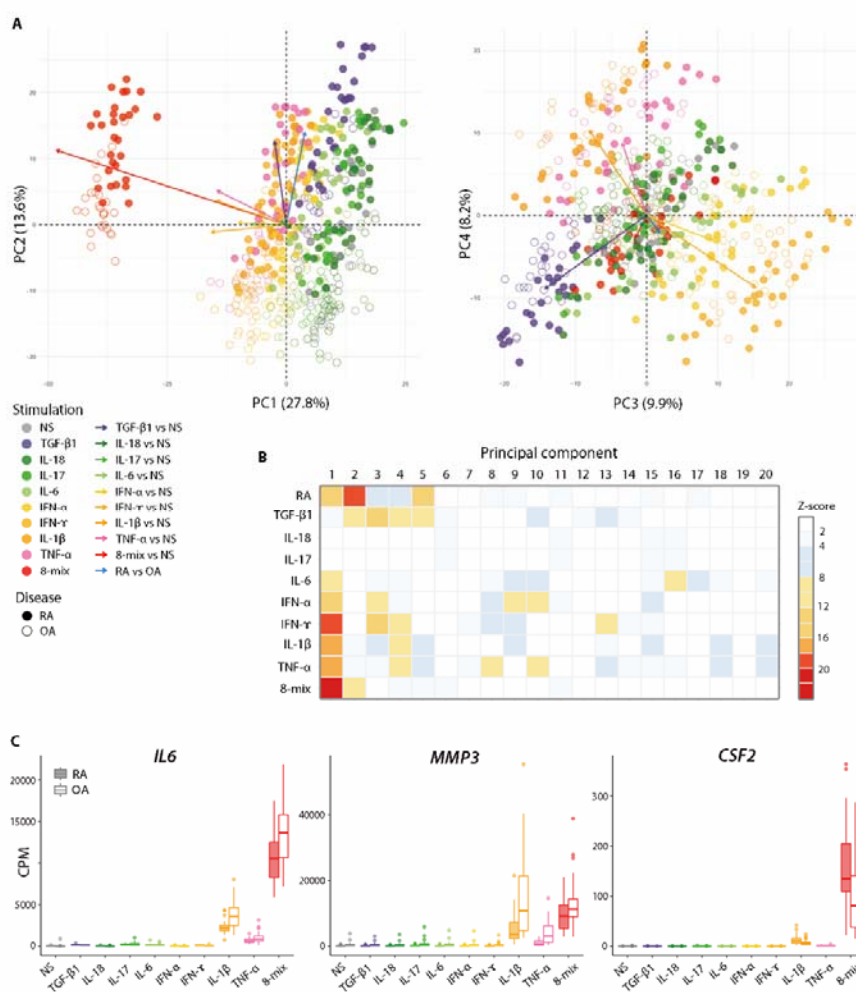OA, osteoarthritis; NS, non-stimulated.

Fig. 2. A distinctive transcriptome signature in SFs induced by the mixture of 8 cytokines.

(**A**) Principal Component Analysis (PCA) of gene expression levels for the top 1000 variable genes.

Samples projected onto PC1/PC2 (left) or PC3/PC4 (right). Numbers in parentheses indicate

contribution ratio (percentage of variation) of the first 4 PCs. Arrows link the centroid of indicated

groups and adjusted to start from the origin.

47

(**B**) Summary of PCA for top 1000 variable genes. We fit a linear model to each PC (i.e., PC ~

Disease + Stimulation). Then we transformed the *P* values to normal Z-scores.

(**C**) Transcript abundances of representative RA pathogenic genes (*IL6*, *MMP3* and *CSF2*) from

RNA sequencing data in stimulated SFs. Boxes, interquartile range; whiskers, distribution; dots,

outliers.

PCA, principal component analysis; RA, rheumatoid arthritis; OA, osteoarthritis; NS,

non-stimulated; CPM, count per million.
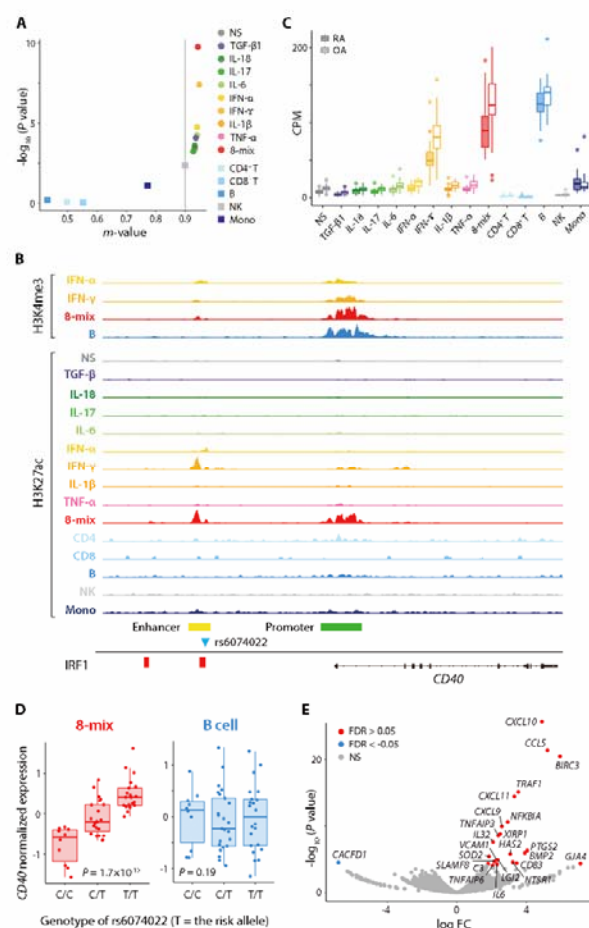
Fig. 3. Stimulation-specific function of RA genetic risk loci.

(**A**) A dot plot of rs6074022-*CD40* cis-eQTL meta-analysis posterior probability *m*-values versus tissue-by-tissue analysis -$\log_{10}$ *P* value. The gray solid line (*m*-value = 0.9) corresponds to the significance threshold in this study.

(**B**) Transcriptional regulatory regions around the *CD40* gene and positional relationship of rs6074022 (blue triangle) in stimulating SFs and PBMCs. IRF1 biding sites were obtained from the

public epigenome browser ChIP-Atras. Data were visualized using the Integrative Genomics Viewer

(IGV).

(**C**) Transcript abundance of *CD40* from RNA sequencing data in stimulated SFs and PBMCs.

(**D**) Expression of *CD40* in SFs stimulated by the 8-cytokine mixture (left) and B cells (right) from

each individual plotted according to the rs6074022 genotype. Nominal *P* values in eQTL mapping

are shown.

(**E**) A volcano plot of differential gene expression analysis comparing the presence or absence of

CD40 ligand (CD40L) for IFN-γ-stimulated SFs. Orange and blue points mark the genes with

significantly increased or decreased expression respectively for the addition of CD40L (FDR <0.01).

Boxes, interquartile range; whiskers, distribution; dots, outliers in (**C**) and (**D**).

RA, rheumatoid arthritis; OA, osteoarthritis; NS, non-stimulated; CPM, count per million.
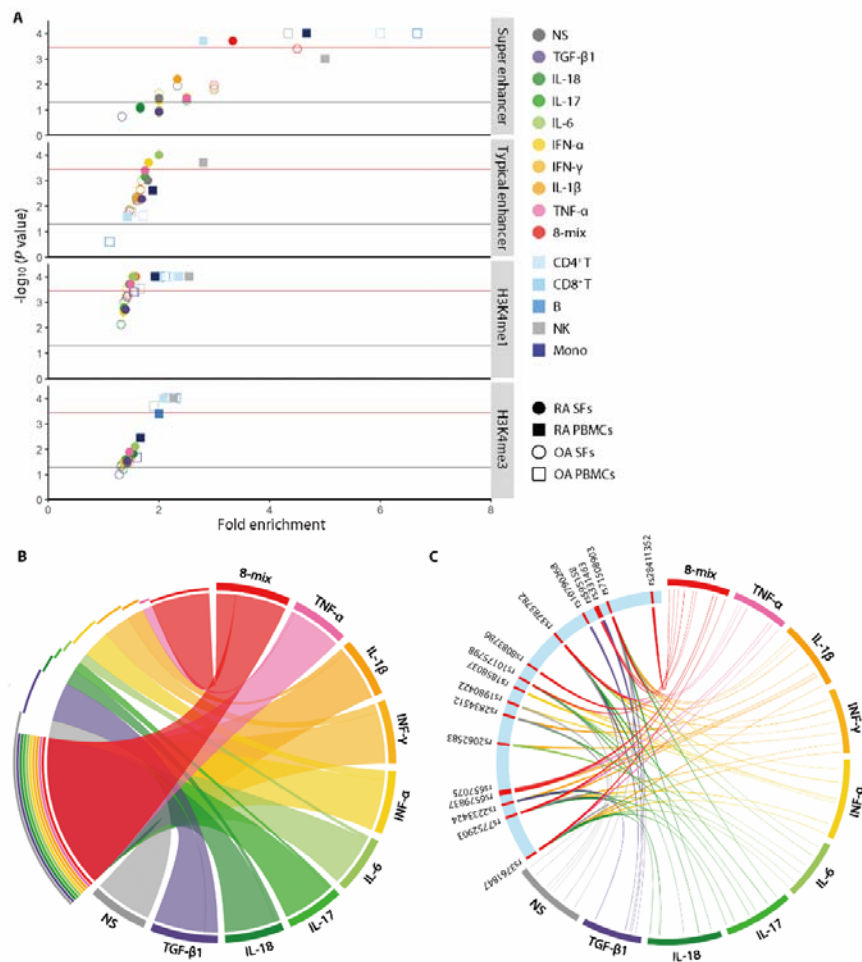
Fig. 4. Enrichment of RA genetic risk in SFs super-enhancers under 8 cytokine stimulation.

(**A**) Enrichment of RA risk loci in transcriptional regulatory regions of stimulated SFs and PBMCs.

Active enhancers were classified into super-enhancers (SEs) and typical-enhancers (TEs) following

standard ROSE algorithms. The red solid lines ($-\log_{10}$ (P value) = 3.2) and the black solid lines

($-\log_{10}$ (P value) = 1.3) are the cutoffs for Bonferroni significance and nominal P = 0.05,

respectively.

51

(**B**) A circus plot showing the overlap of SEs in SFs under different stimulatory conditions. Only the

regions unique to each condition or common to all of the conditions are depicted.

(**C**) A circus plot showing the overlap of RA risk loci and SEs in SFs under different stimulatory

conditions.

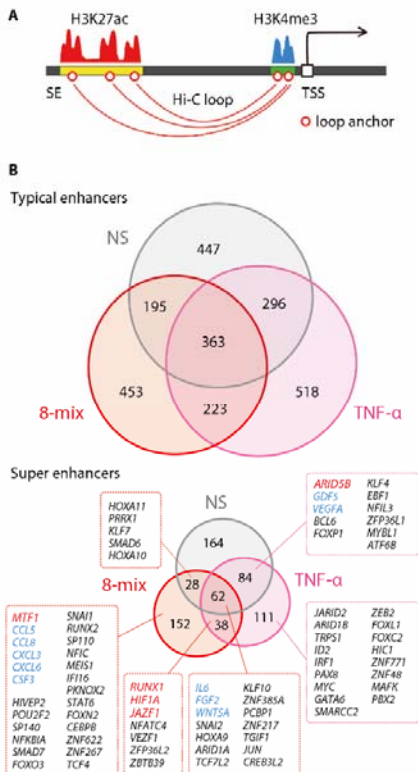NS, non-stimulated; SE, super-enhancer; TE, typical enhancer.

Fig. 5. RA pathogenic factors regulated by SEs in SFs treated with 8 cytokines.

(**A**) A schematic image of "SE-contacted genes".

(**B**) A Venn diagram representing the overlap of TE-contacted (top) or SE-contacted (bottom) genes

in SFs under different stimulatory conditions. Red, blue and black text highlight genes whose

contacted SEs overlap with RA risk loci, cytokines and chemokines and transcription factors,

respectively.

TSS, transcriptional start site; NS, non-stimulated; SE, super-enhancer; TE, typical enhancer.
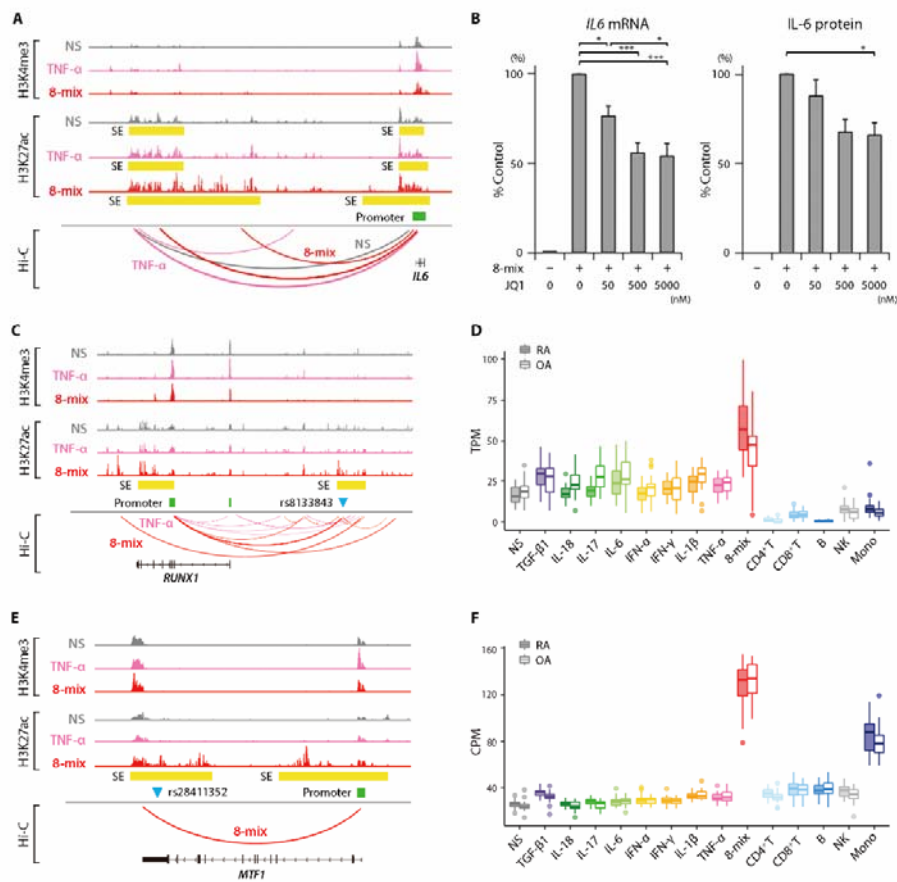
Fig. 6. Representative SE-contacted genes in SFs treated with 8 cytokines.

(**A, C, E**) Organization of transcriptional regulatory regions around *IL6* (**A**), *RUNX1* (**C**) and *MTF1*

(**E**) genes and positional relationship of RA risk loci (blue triangle, rs8133848 for *RUNX1* and

rs28411352 for *MTF1*) and chromatin conformation in stimulated SFs. Data were visualized using

the Integrative Genomics Viewer (IGV).

(**B**) Expression of IL-6 in SFs treated with JQ1. The mRNA and protein expression were quantified

by qRT-PCR (left) and ELISA (right), respectively. Bar graphs, mean; Error bars, SEM. *P* values

54

were determined using one-way ANOVA followed by Tukey's multiple comparison test (*, $P < 0.05$,

***, $P < 0.001$).

(**D, F**) Transcript abundances of *RUNX1* isoform (RUNX1b) (**D**) and *MTF1* (**F**) from RNA

sequencing data for stimulated SFs and PBMCs. Boxes, interquartile range; whiskers, distribution;

dots, outliers.

RA, rheumatoid arthritis; OA, osteoarthritis; NS, non-stimulated; TPM, transcripts per million; CPM,

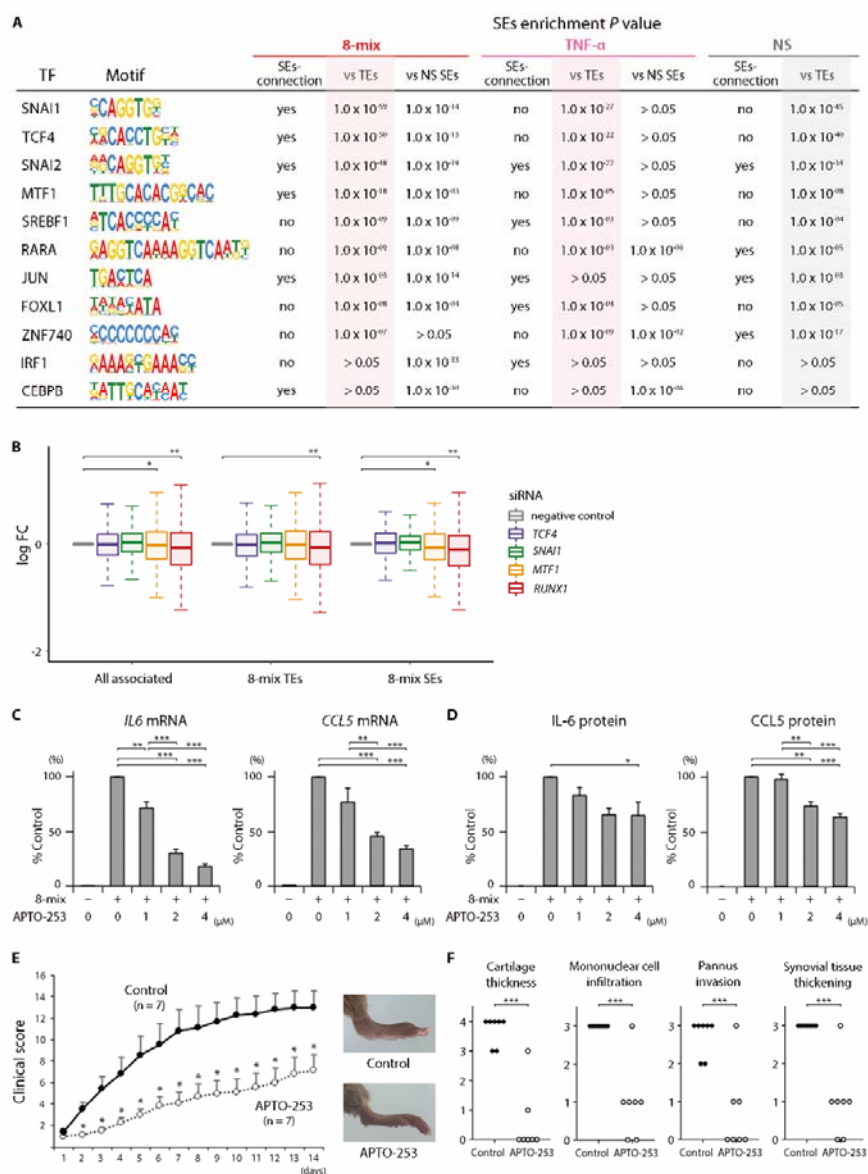count per million; SE, super enhancer.

Fig. 7. Transcription factors associated with stimulation-induced SE formation and arthritis progression.

(**A**) Table depicts transcription factor binding motifs enriched at SEs in stimulated SFs. Following are summarized: attribution to SE-contacted genes, relative enrichment *P* values to TEs in each stimulatory condition or to SEs of non-stimulated condition.

(**B**) Expression of SE- or TE-contacted genes in SFs stimulated by 8 cytokines in cells depleted of specified transcription factors (*TCF4*, *SNAI1*, *MTF1* and *RUNX1*) relative to control SFs. Boxes, interquartile range; whiskers, distribution. *P* values, paired t test (*, $P < 0.05$, ***, $P < 0.001$).

(**C, D**) Expression of IL-6 *and* CCL5 in SFs treated with APTO-253. The mRNA and protein level were quantified by qRT-PCR (**C**) and ELISA (**D**), respectively. Bar graphs, mean; Error bars, SEM. *P* values, one-way ANOVA followed by Tukey's multiple comparison test (*, $P < 0.05$, **, $P < 0.01$, ***, $P < 0.001$).

(**E, F**) Therapeutic effect of APTO-253 on CIA model. Following the onset of arthritis, mice were intravenously injected with either control or 15 mg/kg APTO-253 for twice per day for 2 consecutive days per week. Clinical (**E**) and pathological scores (**F**). Dots, mean; Error bars, SEM. *P* values, Mann–Whitney U test (*, $P < 0.05$, ***, $P < 0.001$).

NS, non-stimulated; SE, super enhancer; TE, typical enhancer.